J Mater Sci (2009) 44:5524–5536
DOI 10.1007/s10853-009-3772-5

A combined synchrotron powder diffraction and vibrational study of the thermal treatment of palygorskite–indigo to produce Maya blue

Manuel Sánchez del Río · Enrico Boccaleri · Marco Milanesio · Gianluca Croce · Wouter van Beek · Constantinos Tsiantos · Georgios D. Chyssikos · Vassilis Gionis · George H. Kacandes · Mercedes Suárez · Emilia García-Romero

Received: 4 May 2009 / Accepted: 22 July 2009 / Published online: 4 August 2009

Abstract The heating process (30–200 °C) of a palygorskite-indigo mixture has been monitored in situ and simultaneously by synchrotron powder diffraction and Raman spectroscopy. During this process, the dye and the clay interact to form Maya blue (MB), a pigment highly resistant to degradation. It is shown that the formation of a very stable pigment occurs in the 70–130 °C interval; i.e., when palygorskite starts to loose zeolitic water, and is accompanied by a reduction of the crystallographic *a* parameter, as well as by alterations in the C=C and C=O bonds of indigo. Mid- and near-infrared spectroscopic work and microporosity measurements, employed to study the rehydration process after the complex formation, provide evidence for the inhibition of the rehydration of MB as compared with palygorskite. These results are consistent with the blocking of the palygorskite tunnel entrance by indigo molecules with a possible partial penetration inside the tunnels. The surface silanols of palygorskite are not perturbed by indigo, suggesting that MB is not a surface complex.

M. Sánchez del Río (✉)
European Synchrotron Radiation Facility, BP 220,
Grenoble Cedex 38043, France
e-mail: srio@esrf.eu

E. Boccaleri · M. Milanesio · G. Croce
Dipartimento di Scienze e Tecnologie Avanzate, Università del Piemonte Orientale, Via Bellini 25/G, 15100 Alessandria, Italy

W. van Beek
Swiss–Norwegian Beamlines, ESRF, BP 220,
Grenoble Cedex 38043, France

C. Tsiantos · G. D. Chyssikos · V. Gionis
Theoretical and Physical Chemistry Institute, National Hellenic Research Foundation, 48 Vass. Constantinou Ave.,
Athens 11635, Greece

G. H. Kacandes
Geohellas S.A., 60 Zephyrou Str., Athens 17564, Greece

M. Suárez
Departamento de Geología, Universidad de Salamanca,
37008 Salamanca, Spain

E. García-Romero
Departamento de Cristalografía y Mineralogía, Universidad Complutense de Madrid, 28040 Madrid, Spain

Introduction

The Maya blue (MB) pigment has attracted the attention of many research groups in the last years. In addition to the continuous interest in the cultural, historic, ethnologic, and archaeological aspects of this pigment invented by the Maya at some time during the first centuries AD [1–3], MB can be considered as a predecessor of modern hybrid complexes [4]. Yet, a long lasting debate concerns the structural and chemical aspects of this organo–clay pigment. The combination of an organic molecule (indigo) with a specific clay mineral (palygorskite) under moderate heating induce some transformations and interactions [5–8] in the indigo molecule that improve the color properties of the resulting complex with respect to bare indigo or the unheated mixture. In this formation process, the color changes from dark blue (indigo) to a more clear turquoise blue, characteristic of the Mesoamerican blue artworks. But the most intriguing aspect of MB is its exceptional chemical stability in concentrated acids, solvents, etc., contrary to indigo which degrades in contact with chemicals or intensive light.

Indigo is one of the oldest dyes used in many civilizations (China, Egypt, Mesoamerica, Europe) formed by

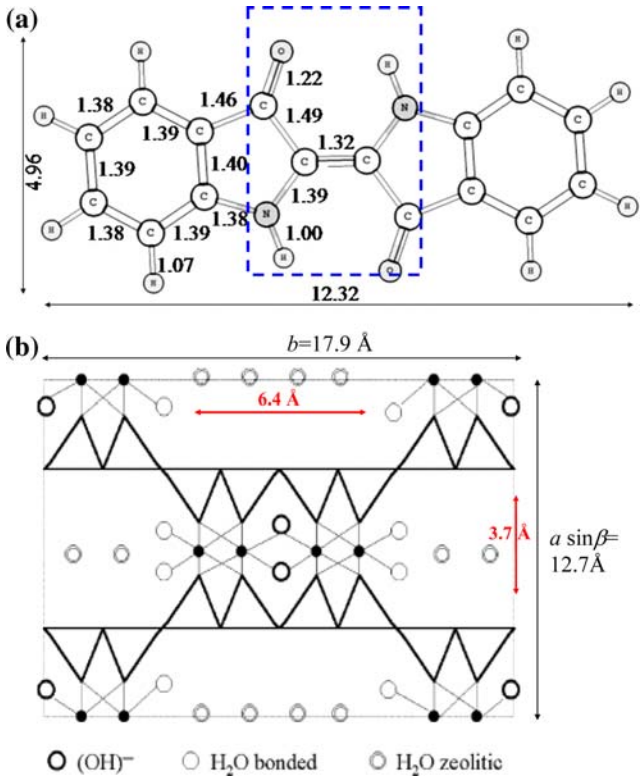

Fig. 1 **a** A schematic representation of the molecule of indigo, with interatomic distances (in Å). **b** A schematic cross section of the palygorskite structure, perpendicular to the direction of the channel. It shows the different types of water. *Triangles* represent the tetrahedral containing Si in the center. *Solid circles* represent the Mg and Al centers. Cell dimensions and tunnel dimensions are also represented (after [47])

indigotin (Fig. 1a) $C_{16}H_{10}N_2O_2$ (3H-indol-3-one, 2-(1,3-dihydro-3-oxo-2H-indol-2-ylidene)-1,2-dihydro), a quasi-planar molecule of approximate dimensions 5 Å × 12 Å. The deep blue color of this organic molecule is attributed to the chromophore shown in Fig. 1a, consisting of one slightly elongated central C=C double bond substituted by two donor groups NH and two acceptor groups –C=O [9, 10]. Both intra- and inter-molecular hydrogen interactions between C=O and NH in the chromophore do affect the hue of the dye, and small atomic or electronic changes may strongly affect the hue. Thioindigo, in which NH groups are replaced by sulfur, shows an intense red color. Monoclinic ($P2_1/c$) crystalline indigo exhibits strong intermolecular hydrogen bonding [11]. Indigo is insoluble in water, and produces deep blue solution in some organic solvents (e.g., pyridine), and sublimes at about 380 °C.

Palygorskite is a fibrous clay mineral of theoretical formula $Si_8(Mg_2Al_2)O_{20}(OH)_2(OH_2)_4{\cdot}4H_2O$. Recent vibrational and analytical data [12] suggest that the composition of palygorskite can be better approximated by the formula $[yMg_5{\cdot}(1-y)[xMg_2Fe_2{\cdot}(1-x)Mg_2Al_2]]\,Si_8O_{20}(OH)_2(OH_2)_4{\cdot}4H_2O$, where x is the Fe-content of the dioctahedral component, and y is the trioctahedral fraction. Palygorskite is a 2:1 phyllosilicate with a modulated structure. The periodical inversion of the apical oxygen of the tetrahedral ions every two silicate ribbons results in a discontinuous octahedral sheet and produces structural tunnels with a 6.4 Å × 3.7 Å cross section (Fig. 1b). These tunnels are populated by strongly bound coordinated water and weakly bound non-structural zeolitic water. The latter can be released by moderate heating or under vacuum. Zeolitic dehydration is reversible and palygorskite rehydrates very quickly in atmospheric conditions. The discontinuity of the silica sheets makes possible the presence of silanol groups (Si–OH) at the external surfaces. The structural model for palygorskite that is mostly accepted today consists of a mixture of two polymorphs: monoclinic and orthorhombic [13–15]. Sepiolite is a similar modulated clay mineral. It is ideally trioctahedral (magnesian) and exhibits wider channels (10.6 Å × 3.7 Å) than palygorskite.

Synthetic analogues to MB were first produced in the 1960s. Van Olphen [16] obtained stable pigments of indigo with palygorskite and sepiolite, using different recipes. He pointed out that (i) the channel structure of the clay is essential to obtain the acid stability (he failed to obtain stable pigments using plate clays), (ii) the necessity of heating to activate the interaction, and (iii) the effect of the particle size. Although Van Olphen and other authors state that MB (or analogous pigments) can also be made with indigo combined with sepiolite, the pigments made with sepiolite are much less resistant than those of made with palygorskite [8]. Van Olphen suggested a first structural mechanism of complex formation, by the positioning of the indigo molecules along the surface grooves of the clay. And he summarized the question open to debate in the following half-century: "*the precise mechanism of the stabilization of the complexes by heating is not clear*." A second possible structural approach proposed by Kleber et al. [17] would allow indigo to penetrate (partially or deeper) into the clay tunnels. It can be found literature supporting Van Olphen [18–22] and Kleber [13, 23–26] models. More recently, Hubbard et al. [6] suggested the covering of the opening of nano-tunnels by the indigo molecules. The structural aspects of the MB formation should be completed with a model of the clay–organic interaction. It is well agreed that a chemical interaction of the palygorskite–indigo complexes is activated by a moderate thermal treatment, which is responsible for the lightning of the color, from the dark-blue of indigo to a turquoise-greenish color in MB. This process has been monitored by optical spectroscopy [7]. Hydrogen bonding [7, 13] or direct bonding [20, 23] mechanisms have also been proposed. Doménech et al. [5, 27–30] applied a solid-state electrochemical methodology, the voltammetry of micro-particles, to study MB. It provided evidence for the

presence of dehydroindigo, the oxidized form of indigo, in MB samples, thus introducing a new factor for explaining the chemistry of this particular organo–clay hybrid material. They also pointed out that different topological isomers of various indigoid molecules attached to the palygorskite matrix may coexist in MB [31, 32].

This study reports on the synchronous monitoring of the formation of MB from a heated mixture of palygorskite and indigo by in situ X-ray diffraction (XRD) and Raman spectroscopy, as a function of temperature. Mid-infrared (MIR) and near-infrared (NIR) spectroscopies as well as porosity measurements are employed to study the rehydration of MB. Beyond the specifics of the indigo–palygorskite interaction, this study belongs to a broader effort in understanding the formation and properties of hybrid organic–inorganic materials involving layered structures [33].

Materials and methods

Indigo was purchased from Sigma Aldrich, Saint-Quentin Fallavier, France. Palygorskite (formerly attapulgite, name still in use for industrial applications) comes from Ticul, Yucatán, Mexico. This palygorskite has been studied in several works [8, 13, 24, 34]. The particular sample employed in this study is mostly dioctahedral ($y = 0.07$) and exhibits a low level of Fe^{III} for Al substitution ($x = 0.12$), estimated from its NIR spectrum as in Ref. [12]. The mixture of palygorskite equilibrated at ambient conditions and indigo was finely crushed in a mortar.

The in situ simultaneous Raman/XRD experiments were performed at the ESRF in Grenoble on the BM1B SNBL (Swiss-Norwegian beamline, http://www.snbl.eu). A 1-mm diameter capillary was filled with a mixture of Ticul palygorskite and indigo (2 wt%). The capillary was kept open so that water could evaporate during the heating process. The high-resolution XRD data were collected with the standard BM1B setup, using a wavelength of 0.50038 ± 0.00001 Å. A continuous set of diffraction patterns was obtained as a function of time or temperature. XRD scans covered the interval 2–22° in two-theta with a step size of 0.02 and finally summed with 0.01 intervals.

The Raman spectra have been measured with a dispersive instrument (Renishaw inVia) with a 785-nm laser excitation and a 1200 lines/mm grating. A RP10 compact video fiber optic probe with a 100-mm long distance objective focuses the laser on the sample and collects the Raman signal back. The RP10 is equipped with edge filters to suppress the Rayleigh scatter. The Raman spectra were collected using a time accumulation of about 60 s per scan.

The sample holder was a rotating capillary, standard for XRD, and suitable for Raman techniques. Thermal treatments were carried out using a Cyberstar gas blower, controlled by a Eurotherm 902b temperature controller. The time synchronization of the Raman and XRD detectors and of the gas blower was obtained by collecting data in continuum and by recording, in each XRD and Raman data file, the time of the measurement. The temperature ramp was set to 1 °C/min. More details and the Raman/XRD experimental setup and on the data collection strategy are reported elsewhere [33].

MIR spectra (525–4000 cm^{-1}) were measured at ambient conditions using a Fourier transform spectrometer (Bruker Equinox 55), equipped with a single reflection diamond attenuated total reflection (ATR) accessory (DuraSampl IR II by SensIR). Each spectrum represents an average of 100 scans at a resolution of 2 cm^{-1}.

NIR spectra (4000–8000 cm^{-1}) were measured on a Fourier transform spectrometer (Vector 22N by Bruker Optics, Marne la Vallée, France), using an integrating sphere attachment. This accessory is suitable for the diffuse reflectance measurement of 500 mg powder samples contained in sealed or open glass vials. The NIR spectra (averages of 100 scans at a resolution of 4 cm^{-1} and a zero-filling-factor of 2) are measured against a gold mirror for reference.

Microporosity was obtained from adsorption–desorption of N_2 in a Micromeritics ASAP 2010 apparatus. The adsorption–sorption isotherma at 77 K were recorded after degassing the samples at 110 °C during 4 h with a residual pressure less than 10^{-5} μmHg.

Results and discussion

The authors who have reported the synthesis of MB agree in the fact that a heating of the palygorskite–indigo mixture is required for obtaining a resistant pigment. However, there is a large variation in the duration of the heating process (from a few minutes [35] to hours or days) and in the applied temperature (90–100 °C in Ref. [35], 190 °C in Ref. [17] or even 250–300 °C in [16]). Palygorskite alone heated to 130 °C undergoes zeolitic dehydration, a process that has been found to be associated with very specific vibrational spectroscopic, therefore structural, changes [36]. Post and Heaney [15] studied the dehydration behavior of two palygorskites from Alaska and Korea by synchrotron XRD and reported that the removal of zeolitic H_2O results in the decrease in unit cell volume by ca. 1.3% owing to a decrease in the *a*-axis by ca. 0.15 Å and the slight increase in the *b*-axis. In turn, the *a*-axis of ambient palygorskite, that determines the height of the tunnel, is dependent on the composition of the octahedral sheet [37]. Therefore, a detailed investigation of the chemical aspects of MB formation by heating requires the parallel structural and spectroscopic study of the particular palygorskite

employed. This is presented in a first section, where the in situ XRD and Raman monitoring permit to correlate structural and chemical changes during the thermal treatment of the palygorskite–indigo mixture. These results are complemented by MIR spectroscopy. A second section describes the ex situ study of the rehydration of the MB during its cooling to room temperature (RT), combining XRD, MIR, and NIR, as well as porosity measurements.

The heating of palygorskite and palygorskite–indigo to produce MB

The heating process (30–200 °C) of a palygorskite–indigo mixture has been monitored in situ by synchrotron powder diffraction and Raman spectroscopy at the same time. This is complemented by ex situ MIR spectroscopy study.

Comparison of the heating of palygorskite and palygorskite–indigo monitored by synchrotron powder XRD

Twenty-two XRD scans of the pristine Ticul palygorskite were recorded upon heating from 33.7 to 193 °C (Fig. 2a). Although there are no drastic changes in the diffractograms, some differences in peak position, shape, and intensity could be noticed. These changes can be studied at the peaks with low 2θ, where there is no overlapping of reflections. In particular, we analyze the peaks at ca. $2\theta = 2.7$, 4.5, 5.3, and 6.4° corresponding to the 110, 200, 130, and 040 reflections, respectively. The modifications in peak position and intensity are related to the changes in cell dimensions accompanying the zeolitic dehydration [15].

The 110 reflection increases significantly in intensity (56%) and its position shifts from 2.725° ($d_{110} = 10.513$ Å) to 2.739° ($d_{110} = 10.458$ Å) when temperature increases. Interestingly, these trends are not linear (Fig. 3a) but follow a sigmoid curve, which can be fitted with an Error function, giving an inflexion at 100 ± 1 °C for the peak intensity and 108 ± 1 °C for the peak position (the error values are one standard deviation obtained from the covariance matrix of the fitting parameters), and width (full-width-at-half-maximum of its Gaussian derivative) at 59 ± 9 °C for the intensities, and 42 ± 8 °C for the peak positions, thus indicating that most changes happen in the 70–130 °C temperature range.

Similar sigmoid variations for the positions and intensities are observed for the other peaks. The intensity of the 200 peak increases by 96% and its position shifts from 4.455° ($d_{200} = 6.434$ Å) to 4.511° ($d_{200} = 6.353$ Å) with a similar sigmoid trend (fit center 103 ± 2 and 34 ± 7 °C width), manifesting the reduction of the cell parameter a (or $a \sin\beta$ if we consider the monoclinic phase of palygorskite). The 130 peak decreases in intensity (15%) and shifts from 5.308° to about 5.297° when temperature increases. The 040 peak increases in intensity by 9% and shifts from 6.421° ($d_{040} = 4.464$ Å) to 6.403° ($d_{040} = 4.476$ Å), with inflexion at 101 ± 2 °C and width 44 ± 7 °C.

The intensity changes of the studied reflections are highly correlated with their shifts. The large increase in intensity of the 110 peak upon dehydration is due to the enhancement of the electron density contrast as the tunnels become empty [33]. In fact, if one supposes that water is lost at approximately the same rate from the two zeolitic sites, as suggested in Ref. [15], one can simulate the dependence of the peak intensity on the zeolitic water occupation using the orthorhombic palygorskite structure defined in Ref. [14]. In this way, we obtained a intensity versus water occupancy dependence close to a straight line (data not shown), with a total increase in intensity of 59% when passing from the fully hydrated to fully zeolitically dehydrated palygorskite indicating that the 110 peak intensity is depending on the charge density present into the tunnels and then it is a good indicator of the amount of zeolitic water lost. The experimental 110 peak intensity increase is 56%, in good agreement with the theoretical value. However, this peak intensity varies with temperature in a sigmoid trend, therefore manifesting that the elimination of the zeolitic water follows the same sigmoid trend versus temperature.

Some other features are noticed from the data: (i) the 200 peak (~4.5°) is split, perhaps as a result that Ticul palygorskite contains more or less the same proportion of orthorhombic and monoclinic phases [13, 34], and their cell parameters do not match exactly. Its shape changes during heating, as a result of an intensity increase in the rightmost component of the peak. Further discussion of this point will require additional measurements. (ii) The peak with 2θ close to 9° comes from impurities: it is the most intense reflection of calcite (i.e., the 014), (iii) the changes in the broad envelope at $2\theta \sim 9°$, a zone that is highly sensitive to the β angle of the monoclinic phase [14], suggesting also a possible variation of this angle during dehydration [15], (iv) the activation of the tiny 020 peak ($2\theta \sim 3.2°$, $d_{020} = 8.95$Å), probably due to an incipient folding of the palygorskite structure [38, 39]. The effect of radiation damage is not excluded as the cause of this effect, observed at lower temperatures than usual.

A similar procedure was done for the palygorskite and indigo mixture. Twenty-three XRD scans were recorded (Fig. 2b) upon heating from 36 to 199 °C. The variations of the 110 peak intensity and position (Fig. 3b) are similar to those of pristine palygorskite (Fig. 3a), but they are centered at lower temperatures (inflexion of the Error function fit at 80 ± 3 °C for the peak intensity and at 94 ± 2 °C for the peak shift). The increase in peak

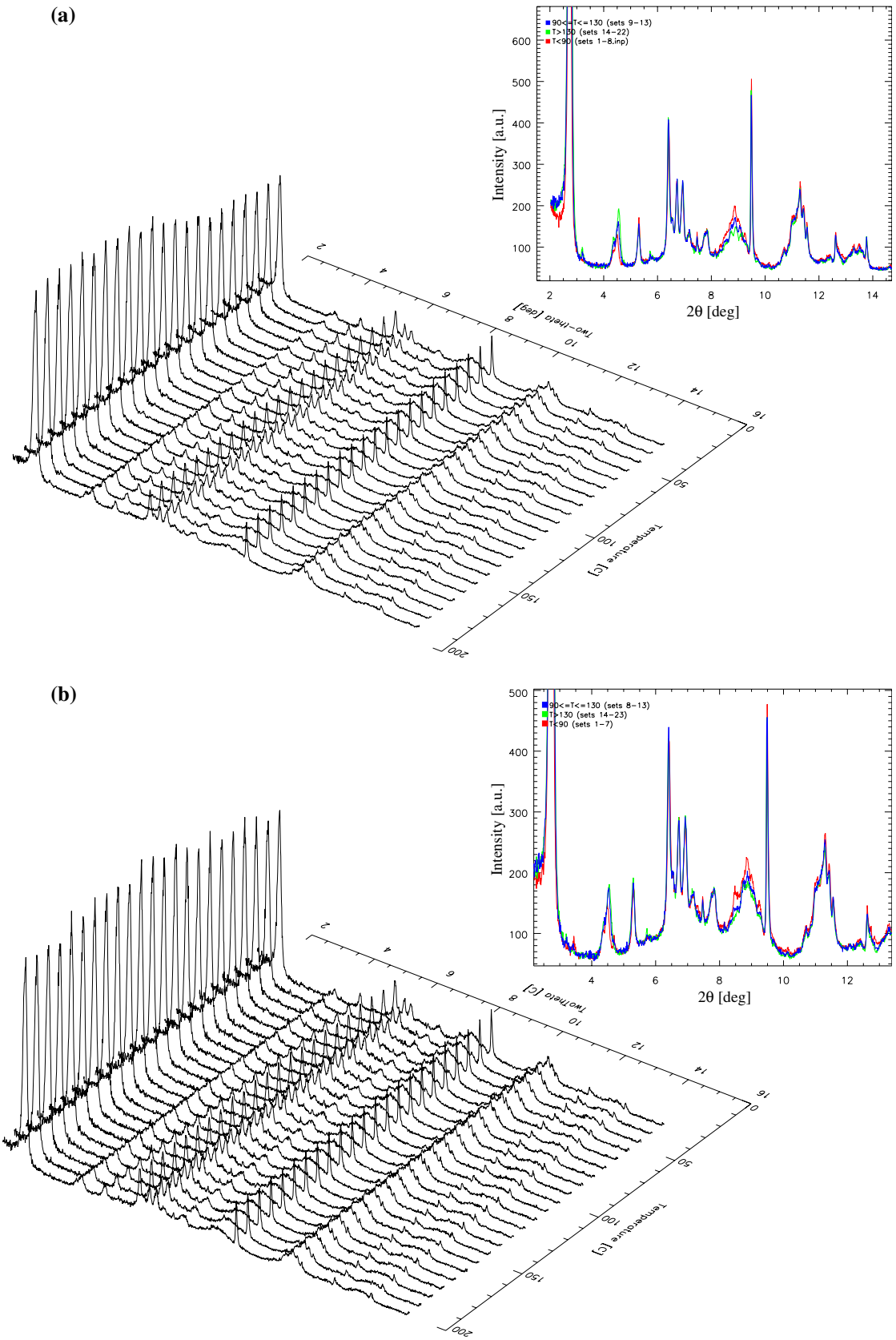

Fig. 2 X-ray diffractograms recoded as a function of the temperature for **a** palygorskite and **b** palygorskite–indigo mixture (1 wt% indigo). *Insets*: X-ray diffractograms averaged in three temperature ranges

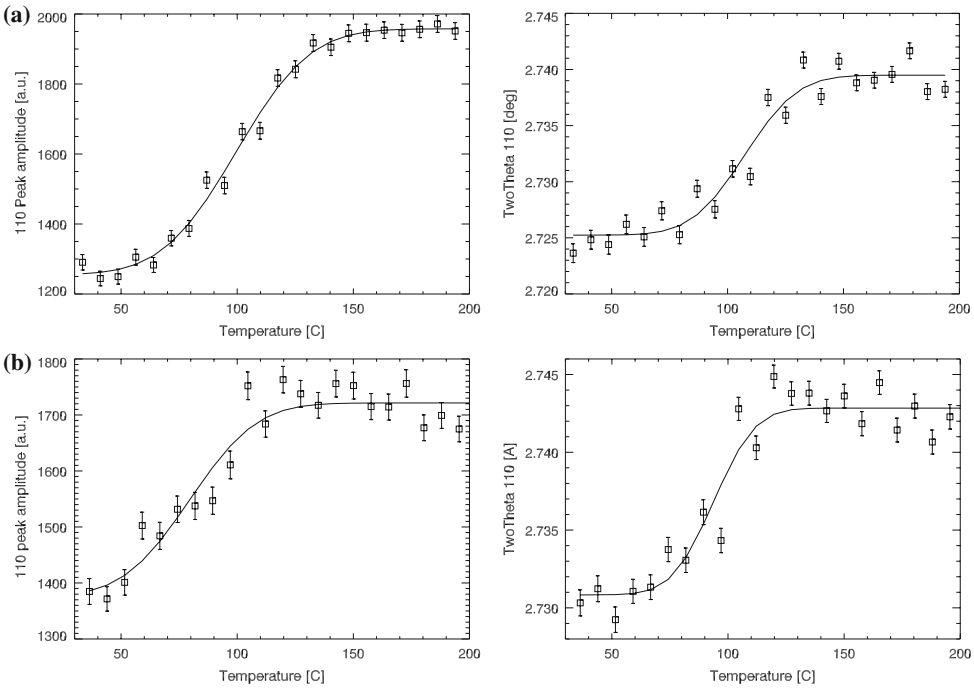

Fig. 3 Evolution of the 110 XRD peak intensity and peak position versus temperature for **a** palygorskite and **b** palygorskite and indigo (1 wt%). Experimental points are fitted with an error function (*continuous lines*)

intensity is much reduced (25%) as compared with pristine palygorskite (56%), indicating that the indigo inhibits the evacuation of the zeolitic water with respect to the same heating treatment in pristine palygorskite and/or that indigo enters the tunnels and reduces contrast.

The 200 peak increases 65% its intensity and shift from 4.462° (d_{200} = 6.422 Å) to 4.512° (d_{200} = 6.351 Å) with a similar sigmoid trend (fit center 89 ± 3 and 39 ± 10 °C width). The 130 peak increases 16% its intensity and shifts from 5.309° to 5.295° when temperature increases. The 040 peak slightly increases its intensity and shifts from 6.422° (d_{040} = 4.464 Å) to 6.403° (d_{040} = 4.476 Å), with inflexion in 96 ± 2 °C and width 38 ± 6 °C.

Therefore, the total changes in cell parameters in MB are similar to pristine palygorskite: a (or $a \sin\beta$) decreases by 0.14 Å upon MB formation (0.16 Å for pristine palygorskite) and b increases slightly (0.05 Å for both MB and pristine palygorskite). These changes are related to the loss of zeolitic water in both cases, and in good agreement with Ref. [15]. There are, however, small differences: the inflexion point is found at slightly lower temperatures in MB than in pristine palygorskite. This may be explained by a blocking of the dehydration process at a given moment because of the presence of indigo. In the absence of indigo, the palygorskite continues to dehydrate, thus the inflexion of the sigmoid curve is found at slightly higher temperatures. The increase in the peak value of the 110 reflexion versus temperature is much more important in the case of palygorskite than in indigo. Also, the smaller increment of the cell parameter a in MB with respect to pristine palygorskite is compatible with the idea that the dehydration in MB is obstructed by indigo as well as with the idea of indigo entering into the tunnels. This may be the result of the partial introduction of the indigo in the palygorskite tunnels or blocking of the tunnel entrances, with a double effect: the release of zeolitic water is inhibited, and the electron density of the palygorskite matrix is altered, thus reducing the diffraction signal.

In order to better visualize the changes in temperature, we averaged (i) the diffractograms for $T < 90$ °C that remain almost constant, (ii) the diffractograms for $T > 130$ °C also constant, and (iii) the diffractograms for temperatures in the 90–130 °C range which are those that change the most. They are represented in the insets of Fig. 2. Similar trend is obtained for MB than for palygorskite with the exception of some tiny peaks (2θ = 3.44°, 4.71°, and 7.32°) that correspond to crystalline indigo, and are only visible at low temperatures.

In situ Raman monitoring of the heating of a palygorskite–indigo mixture

The study of MB by Raman spectroscopy has the advantage that only indigo is active, therefore it simplifies the interpretation with respect to infrared spectroscopy, where indigo and palygorskite bands are superimposed. Palygorskite can be seen in the Raman spectrum using NIR excitation [40]. The Raman spectrum of MB is similar, but

not identical, to that of indigo. In fact, several bands of the MB spectrum are different to those of indigo. Witke et al. [41] remarked the presence of new bands in MB and an intensity increase in some indigo bands. They suggested that the indigo molecule losses its planarity when interacting with palygorskite, this mechanism being responsible of the exceptional stability of MB. Sanchez del Rio et al. [42] showed that similar differences between indigo and MB do occur in the non-heated palygorskite–indigo mixture, which is not resistant to acids. Moreover, they found similar effects with indigo–sepiolite, and indigo mixed with other planar clays, which do not form stable pigments. Therefore, the interest here is not to compare the Raman spectrum of MB with the indigo spectrum, but to study the differences in Raman spectra when the palygorskite–indigo mixture is being heated. The Raman spectra from the in situ coupled Raman–XRD measurements are shown in Fig. 4. The changes in the position and intensity of peaks in the Raman spectra are discussed in four wavenumber zones based on the band assignation by Tatsch and Schrader [43] and Sanchez del Rio et al. [42].

The first zone (<200 cm^{-1}) corresponds to lattice vibrations of the indigo. We observed (Fig. 4) three peaks at RT (135, 172, and 182 cm^{-1}) with linearly decreasing intensities as temperature increases until they totally disappear around 100 °C. This is due to the excess of crystalline indigo that disappears with temperature, because its crystalline structure is lost when it diffuses and interacts with palygorskite. This is in well agreement with the extinction of the indigo peaks in XRD.

The second zone (200–590 cm^{-1}) is related to the in-plane bending (δ) and out-of-plane deformation (γ) modes of several groups containing the double bonds present in indigo (C=C, C=O). The complex envelope in the 200–300 cm^{-1} range is heavily altered by the thermal treatment. We observe four peaks in this region: 237 cm^{-1}

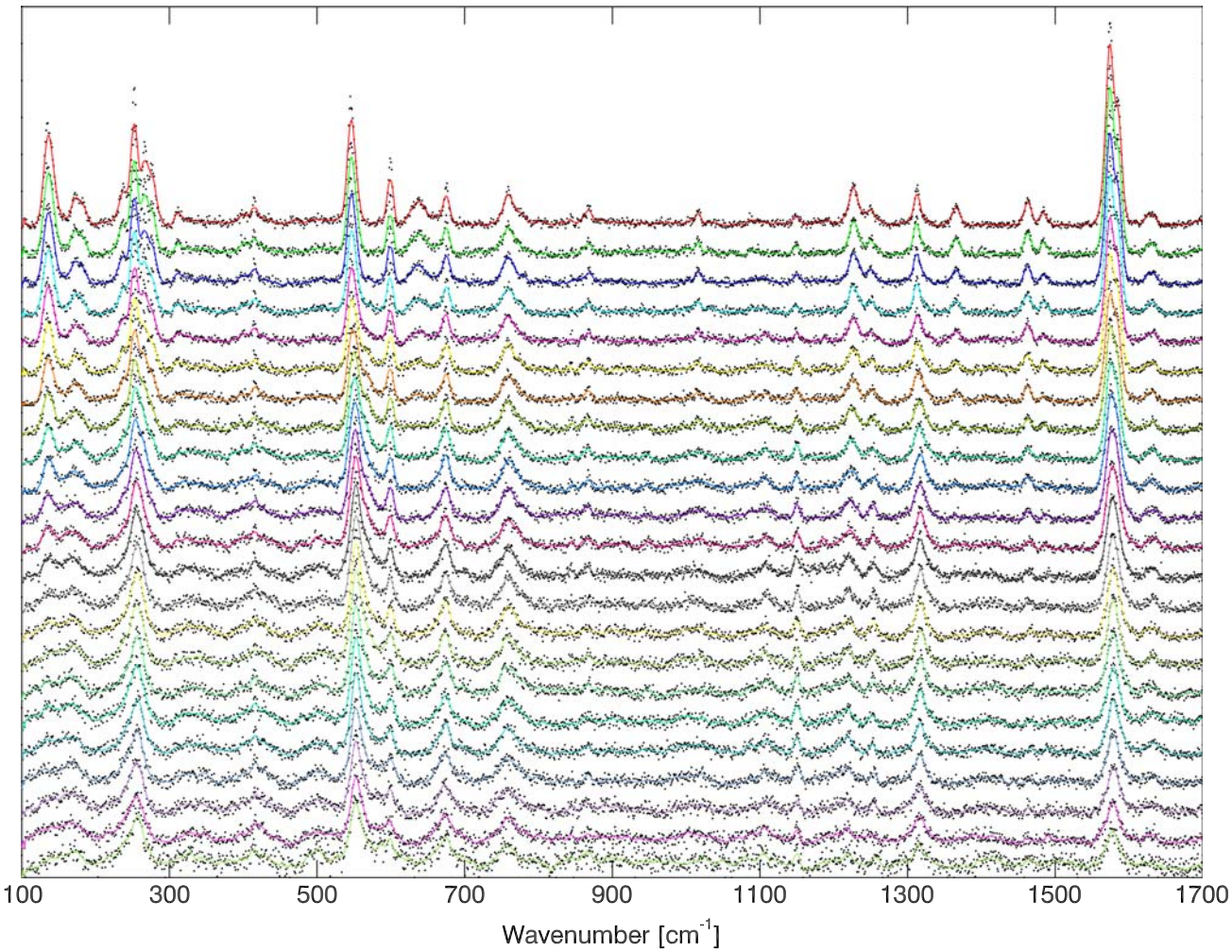

Fig. 4 Raman recoded as a function of the temperature for palygorskite and indigo (1 wt%). Spectra are shifted vertically for clarity. The *points* represent the (averaged) experimental points and the *continuous lines* are the smoothed data. The spectra, from top to bottom, go from RT (T = 36 °C) to T = 199 °C

unassigned in Ref. [43], 253 cm^{-1} corresponding to out-of-plane vibrations of the double bonds C=C and C=O and the 266 plus 275 cm^{-1} peaks that are assigned to in-plane vibrations of the double bonds possibly including the five-member ring. With increasing temperature, these four peaks merge in a single broadband. The variation with temperature follows a similar trend as observed in the XRD case: the four peaks are well resolved for $T < 90$ °C, all they merge in a large band in $90 < T < 130$ °C and this band remains almost constant for $T > 130$ °C (its width increases slowly with temperature). Nagasawa et al. [44] found that indigo carmine in protic solvents presents a single broad peak at ~ 260 cm^{-1}, whereas it become a doublet (254 and 265 cm^{-1}) in aprotic solvents. Therefore, we could make a parallelism of the transition from unheated to heated palygorskite–indigo with the passage from aprotic to protic solvents. An intense band at 547 cm^{-1} corresponds to in-plane vibrations δC=C–CO–C. This band shifts 7 cm^{-1} to higher wavenumbers with temperature (Fig. 5). The trend is again sigmoidal and fitted with an Error function (inflexion at 85 ± 1 °C and width 42 ± 3 °C). These values are similar to those of the variation of the XRD 110 peak position (Fig. 3, inflexion at 94 ± 2 °C and width 33 ± 6 °C). The C=C–CO–C group contains the chromophore of the indigo molecule, therefore it is deduced that the active part of the indigo interacting with the clay is here. The interaction shown here runs parallel to the bathochromic shift observed in optical spectroscopy from indigo to MB [7]. The good correlation of the peak shift between XRD and Raman data as a function of temperature indicates that the chemical interaction occurs when the palygorskite cell parameter a is reduced, with a possible indication of the trapping and immobilization of the indigo molecule in the tunnels, or in the tunnel entrances.

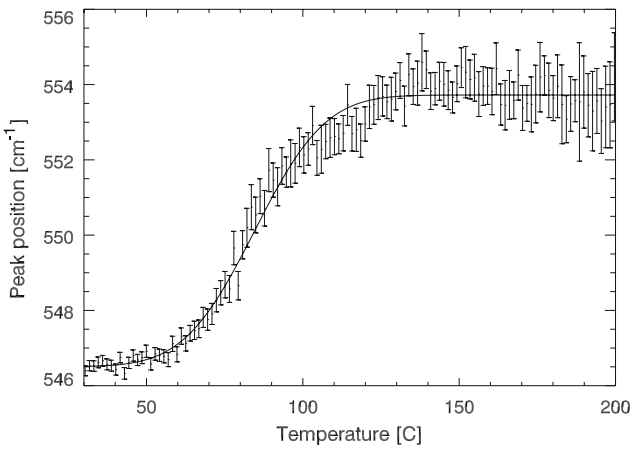

Fig. 5 Change in position versus temperature of the δC=C–CO–C band for palygorskite and indigo (1 wt%)

The third zone, in the 590–1100 cm^{-1} range, refers to bending and deformations of C bonds. It may occasionally contain some information on double C=C and C=O bonds, and does not include stretching modes. The band at 599 cm^{-1} losses 75% of its intensity linearly with temperature, with no change in position. After Tatsch and Schrader [43], this peak corresponds to δC=O δC–H and δC–NH–C, but Sanchez del Rio et al. [42] assigned it to δC–C_{ring} and δC–N. The fact that this band does not shift with temperature, as it happens for those involving a double C=C or C=O bond, suggests that there is no double-bond involved, as suggested in Ref. [42]. The decrease in intensity may be given to the role of NH, as discussed below.

A broad band at 636 cm^{-1} corresponds to out-of plane vibrations γN–H [43] with some minor contribution of C–C [42]. The intensity of this band decreases linearly with temperature, and vanishes above 120 °C, without shifting. Leona et al. [45] suggested that this band, which is present in indigo and absent in MB, can be used for the unambiguous differentiation of pure indigo from its form fixed on palygorskite. Although this band is seen here at low temperatures, Sanchez del Rio et al. [42] do not find it in unheated mixtures of indigo with palygorskite, sepiolite, and montmorillonite. The fact that it disappears quickly before the crucial temperatures in the range $90 < T < 130$ °C can be explained by two facts. The first one is related to a loss of planarity of the indigo molecule when interacting with the clay surface. For the Raman spectra of indigo carmine in solution [44], this peak is sharp and strong with aprotic solvents, and broad and weak with protic solvents. This clay–indigo interaction at the surface occurs even before applying the thermal treatment, and is common to indigo with several clays, including laminar ones. Therefore, although this surface interaction may exist in MB, it is certainly not responsible of its resistance. The second explanation is related to an excess of indigo. It is clear that the vibrations of the N–H bond do change when passing from indigo to MB, because in pure indigo there are inter and intra-molecular interactions (hydrogen bonding) of N–H with C=O, which are certainly altered when the crystalline structure is lost, but we believe that the N–H group is not involved in the mechanism that produces stability to MB. This idea is also supported experimentally by the fact that a stable pigment can be made with palygorskite and thioindigo, which does not contain NH. Interestingly, a thioindigo–palygorskite mixture turns from red to deep blue when heating, similar to what happens with 44′–77′-Tetracloroindigo [7].

The band at 675 cm^{-1} (a complex in-plane vibration mode [42] mixing δC–C_{ring}, δN–H and perhaps double bonds C=C, C=O) doubles its width linearly when passing from RT to 200 °C, with a slight linear shift to lower

wavenumbers (~ 2 cm^{-1}) but keeping constant its amplitude. The band at 759 cm^{-1} (δC–H and δN–C–C [43]) becomes ca. 50% broader when temperature increases, but it does not shift. Three small peaks are also observed: (i) at 868 cm^{-1}, with amplitude that slightly decreases with temperature but does not disappear at high temperatures, (ii) 1016 cm^{-1} which intensity reduces quickly and disappears at 100 °C, and (iii) 1090 cm^{-1} that also disappears at <100 °C. These peaks correspond to indigo bands [43], but they are too noisy in our data to discuss possible shifts.

The fourth and last zone corresponds to wave numbers in the region 1100–1700 cm^{-1}. We found ten bands all of them listed in Refs. [42] and [43]. The two vibrational bands including nitrogen reduce their intensity with increasing temperature: (i) the 1227 cm^{-1} band (δC–H, νC–N after Ref. [43]) decreases ca. 30% of its intensity linearly from RT to 70 °C, then it becomes constant. It shifts to lower wave numbers (~ 8 cm^{-1}) in the temperature range 70–200 °C. (ii) The 1364 cm^{-1} band (δN–H δC–H after Ref. [43]) disappears linearly with temperature until a total extinction at $T \sim 120$ °C. Two bands are related to double bonds: (i) 1250 cm^{-1} (δC–H δC=O after Ref. [43], or δC–H δC=C δN–H after Ref. [42]) shifts to higher wave numbers (~ 4 cm^{-1}) with a sigmoid trend, and (ii) 1313 cm^{-1} (δC–H δC=C after Ref. [42]) increases its intensity ca. 50% and shifts to higher wave numbers (~ 5 cm^{-1}) with a sigmoid trend, keeping a constant width. The peaks at 1574 cm^{-1} (νC–C [43] or δN–H δC–H $\delta\nu$C–C_{ring} [42]) and 1585 cm^{-1} (stretching modes of the C=C and C=O bonds [43]) overlap in a doublet. This doublet at RT broadens and appears as a single band at ca. 1579 cm^{-1} upon MB formation. Similar spectral differences between indigo and MB have been observed by Leona et al. [45], ascribed to modifications in the charge distribution of the indigo molecule during its fixation to palygorskite, together with the disappearance of the signal due to intermolecular interactions in free indigo. Moreover, these authors suggested that the shifts in N–H and C=O frequencies can be explained with different hydrogen bonding for these functional groups in pure indigo and MB, without excluding a possible change in symmetry. Our spectra show that the doublet intensity slightly decreases and becomes broader when increasing temperature.

Some conclusions can be withdrawn, even though the peak overlapping makes difficult to quantitative analyze each peak of the Raman spectrum independently, and the inherent noise in the in situ Raman recording. The peaks related to N–H tend to disappear linearly with temperature, because they are highly affected by the loss of crystallinity in indigo, a phenomenon that occurs when the indigo molecule interacts with the clay, even if the interaction is only at the clay surface. Therefore, this group does not play an essential role in the stability of MB. This has been noticed by numerical simulations using molecular dynamics [23] and it is reinforced by two experimental facts: (i) a resistant pigment can be obtained with thioindigo, which does not contain N–H, and (ii) similar indigo–palygorskite hydrogen bonding through NH should also occur in sepiolite–indigo, and well in indigo with other planar clays, where the mineral presents similar termination groups; however, it is well known that the resistance of palygorskite–indigo is much superior than for the other complexes [8]. Other peaks corresponding to C–C and C–H present changes in amplitude and shifts, but no direct conclusions can be drawn. The position of the stretching and in-plane bending vibrations that include double bonds C=C and C=O changes following a sigmoid curve, similar to what is observed for the intensity of the 110 XRD peak. This indicate that the electronic changes that occur in the indigo chromophore when interact with palygorskite do happen when the tunnel shrinks. It could be visualized as if the height of the palygorskite tunnel starts to close, trapping, and fixating the indigo molecule at the entrance of the tunnel. Results of other complementary experimental techniques are in well agreement with hypothesis, as shown below.

MIR analysis of palygorskite and palygorskite–indigo

As discussed earlier, Raman spectroscopy does not provide information about the structure of palygorskite and its possible changes associated with the formation of MB. For this reason, we compare the infrared absorption spectra of palygorskite and a 5 wt% indigo–palygorskite mixture before and after heating to 130 °C (Fig. 6). A higher indigo

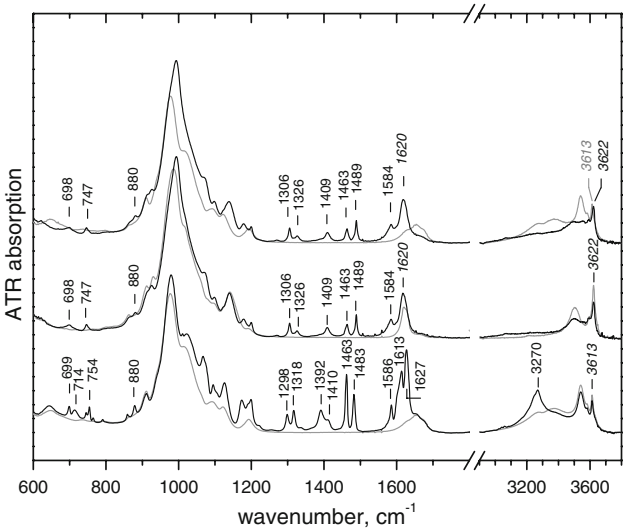

Fig. 6 ATR spectra of palygorskite (*gray*) and indigo–palygorskite 5 wt% mixture (*black*). *Bottom*: No thermal treatment, equilibrated to ambient conditions. *Middle*: Immediately after heat treatment at 130 °C overnight. *Top*: Heat-treated samples re-equilibrated to ambient conditions for 1 h

concentration has been chosen for infrared experiments with respect to Raman experiments in order to be more sensitive to the changes induced by the indigo. The spectrum of the unheated mixture is the superposition of the spectra of hydrated palygorskite [36] and polycrystalline indigo [43], suggesting that simple grinding of palygorskite with indigo does not alter the structure of the latter. Zeolitic dehydration by heating to 130 °C has a very characteristic effect on its infrared spectrum [36]. Changes involving the stretching and bending modes of water (3000–3600 and 1600–1650 cm^{-1}, respectively), the envelope of the Si–O stretching modes (950–1200 cm^{-1}) as well as the blue-shift of the AlAlOH stretching mode from 3613 to 3622 cm^{-1}, are observed in both heated palygorskite and MB. This suggests that the presence of indigo in MB does not induce any significant structural changes to palygorskite, as this exhibits the expected pattern of zeolitic dehydration. On the contrary, and in agreement with the Raman data, the indigo-diagnostic part of the infrared spectrum undergoes changes in peak positions and relative intensities that are typical of MB formation. We are therefore faced with a situation where the specific chemical interaction between indigo and palygorskite leading to the formation of MB is easily detected from the spectra of indigo itself, but has little or no effect on the spectra of palygorskite. This can only imply that this interaction involves a small part of the active (surface or tunnel) sites of dehydrated palygorskite, and therefore remains below the detection limits of our techniques.

Similar studies have been carried out using different indigo–palygorskite concentrations. They indicate that the palygorskite–indigo signatures found below are maintained from 1 to more than 5% and less than 10% of indigo in palygorskite. Obviously, a higher indigo concentration produces a darker pigment.

Study of the rehydration of palygorskite and palygorskite–indigo

The formation of MB implies a heating of the palygorskite–indigo mixture, as studied in the previous paragraph. However, a second unavoidable phase is the cooling back to RT, whose effects are studied here. It is well known that, after moderate heating to evacuate zeolitic water, the raw palygorskite rehydrates quickly by just absorbing atmosphere water vapor. The interaction with indigo suggests a clear distinction between neat palygorskite and MB when the zeolitically dry samples are left to rehydrate in the ambient.

In order to study the rehydration of the MB by XRD, we have heated ex situ to 200 °C a capillary with palygorskite–indigo mixture in an oven, then seal the capillary at 200 °C, cool to RT, put it in the beam, broke the capillary to allow rehydration, and take four measurements after the capillary has broken (about 20 min). The diffractograms obtained did not change with time, meaning that there is no rehydration when the pigment is put in contact with the atmosphere. This is shown by calculating the difference diffractograms (Fig. 7) where the smaller difference is found with $T > 130$ °C, indicating that the sample is not rehydrated after the formation of MB. Notice, however, a largest difference in the negative values close to the 110 peak position, meaning a change in peak width, and some large differences around 15°, which may be affected by noise. For the calcite peak ($2\theta \sim 9.4°$) it is found a larger difference with the high temperature one (green line), due to the fact that calcite is not affected by water and there is only the effect of the thermal expansion/compression of the unit cell.

The MIR spectra of Fig. 6 indicate that a 10-mg sample of dehydrated neat palygorskite rehydrates fully and within minutes after exposure to ambient. The Si–O–Si bands (1000–1200 cm^{-1}) are sensitive to expansion of the *a*-axis upon rehydration in palygorskite, but this effect is not seen in MB, in good agreement with the XRD previously discussed. Also, the AlAlOH stretching band shifts in the palygorskite spectrum from its dehydrated position (3622 cm^{-1}) to its ambient position (3613 cm^{-1}) but not for MB. Therefore, in agreement with the XRD data, the 5% indigo MB preparation remains zeolitically dry after a 1-h exposure to the ambient (Fig. 6), suggesting that indigo is blocking the entrance of water inside the palygorskite tunnels.

A more detailed vibrational spectroscopic assessment of palygorskite in MB can be obtained from the second derivative NIR spectra in the OH stretching overtone region (Fig. 8). The use of the second derivative ensures

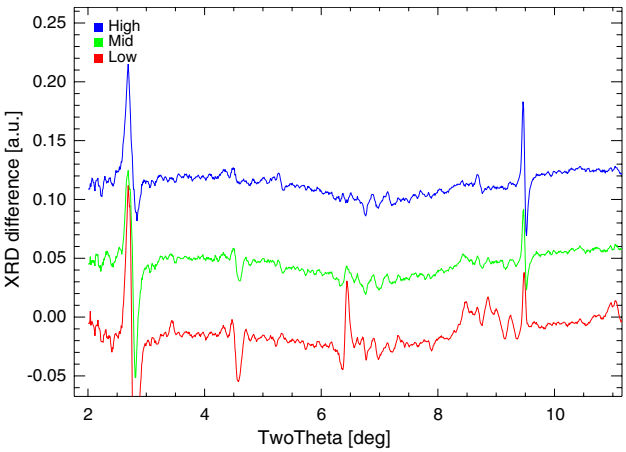

Fig. 7 Effect of possible rehydration of MB. The figure shows the differences between the averaged diffractogram during rehydration and the averaged diffractogram for *low* temperatures $T < 90$ °C (*bottom*), the averaged diffractogram for *mid* temperatures $90 < T < 130$ °C (*center*), and the averaged diffractogram for *high* temperatures $T > 130$ °C (*top*)

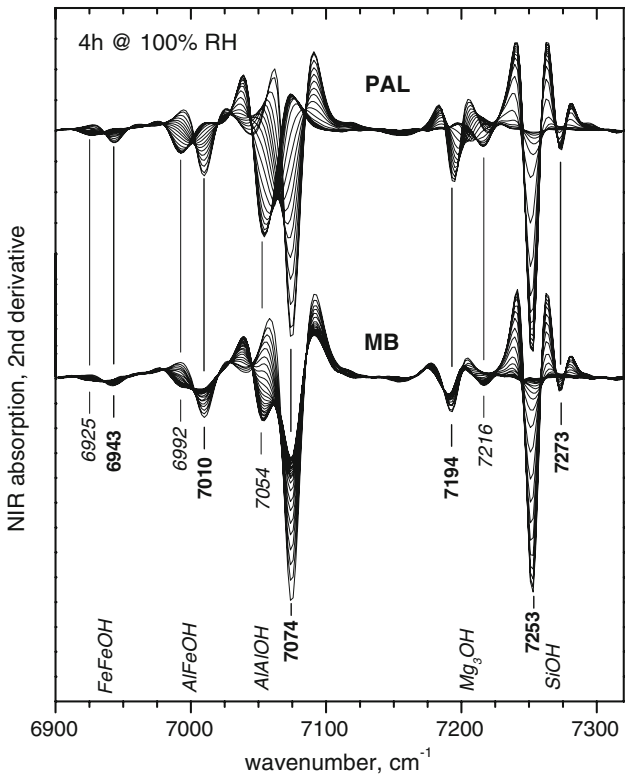

Fig. 8 NIR second derivative real-time monitoring of the rehydration of neat palygorskite (*top*) and a 5 wt% mixture of indigo–palygorskite (*bottom*) heated to 130 °C overnight and during a 4 h equilibration to ambient temperature and 100% RH. Spectra are shown in the OH overtone region. The main peaks of the dehydrated and rehydrated phases are marked in *bold* and *italics*, respectively

that the broad bands due to the stretching modes of the various types of H_2O are filtered out, leaving behind very clear signatures of AlAlOH, AlFeOH, FeFeOH species of dioctahedral palygorskite (7054, 6992, 6925 cm^{-1}, respectively), and Mg_3OH groups of trioctahedral palygorskite (7216 cm^{-1}) [46]. Upon zeolitic dehydration, the dioctahedral triplet exhibits a blue-shift by ca. 20 cm^{-1}, whereas the trioctahedral mode shows an opposite shift. Therefore, the position of the overtones of the structural hydroxyls is a sensitive indicator of the strain induced on the modulated 2:1 layers by the removal of zeolitic H_2O. Zeolitic dehydration is accompanied by the dehydration of the external surface silanol groups (SiOH), which is manifested by the appearance of new sharp bands at ca. 7250 and 7270 cm^{-1} [36]. The spectra of neat palygorskite and 5 wt% MB samples (500 mg each), sealed and measured immediately after heating to 130 °C, are found identical in terms of both structural and surface OH groups (Fig. 8). However, the two samples exhibit drastically different rehydration behavior upon exposure to 100% RH at ambient temperature. The rehydration of the neat sample involves the expected one-mode shift of the structural hydroxyls and the concomitant disappearance of the discreet SiOH features [36]. On the contrary, the rehydration of the MB sample under the same experimental conditions is more complex. While the surface SiOH groups rehydrate freely as in neat palygorskite and the intensity of their NIR active overtone vanishes, the relaxation of the structural hydroxyls toward their normal "hydrated" position is only partial: about half of the structural hydroxyls rehydrate freely but the remaining half do not, suggesting that about 50% of the channels are blocked. Further experiments (data not shown) demonstrate that the rehydration of MB does not advance significantly after ca. 1 month at 100% RH. The fraction of blocked channels is a function of the indigo content: it is not more than ca. 10% in 1 wt% indigo MB but can be as high as ca. 70% in 10% indigo MB.

The micropore surface is calculated for raw palygorskite and unheated and heated (190 °C during 5 h) by measuring the adsorption–desorption of N_2. The results (Table 1) show that (i) the porosity of the raw palygorskite and the palygorskite heated at 190 °C during 5 h (then rehydrated naturally in the atmosphere) present identical values, demonstrating that the thermal treatment applied does not affect the palygorskite porosity, once this palygorskite is fully rehydrated. The unheated palygorskite–indigo samples present smaller porosity, due to the presence of the large indigo molecules that block the pores. Moreover, this blockage is even increased after the thermal process, making irreversible the reduction of the micropore surface. This is in good agreement with the microporosity data from [6], and supports the idea of a partial filling of the zeolitic tunnels in MB.

Table 1 Surface BET, external surface, and microporous surface obtained from the isotherms of the adsorption–desorption of N_2

Sample	BET surface (m^2/g)	External surface (m^2/g)	Micropore surfaces (m^2/g)
Unheated palygorskite	236 (221)	124 (140)	112 (81)
Heated (5 h 190 °C) palygorskite and ambient rehydration	236 (224)	120 (131)	116 (93)
Unheated palygorskite (Ticul) + 1% indigo	273 (185)	187 (124)	86 (61)
Heated (5 h 190 °C) palygorskite + 1% indigo and ambient rehydration	153 (175)	111 (120)	42 (55)

Numbers in brackets correspond to samples prepared using Attapulgus palygorskite instead of Ticul palygorskite (no brackets)

The fact that MB does not rehydrate as fully as palygorskite does mean that water is obstructed from entering the channels, thus supporting the idea that the indigo molecules block the entrance to the tunnels, either by the trapping of a single (or cluster) of indigo molecules at the opening of the tunnels or by the partial penetration of several indigo monomers into the tunnels, which is never completely free of zeolitic water.

Summary and conclusions

A mixture of palygorskite and indigo has been heated from RT to about 200 °C under synchrotron XRD and Raman monitoring. The XRD shows a reduction of the *a* cell parameter of 0.16 Å due to the loss of zeolitic water. This effect, similar for raw palygorskite and palygorskite–indigo, occurs in the temperature interval 70–130 °C. Raman spectra evidenced changes in the same temperature interval at the vibrations involving the double bonds C=C and C=O, indicating that the modification of the indigo chromophore is correlated with the shrinking of the tunnel width. The palygorskite–indigo mixture does not rehydrate after being heated as raw palygorskite does. The rehydration in MB was studied by MIR, NIR, and microporosity, and the data are fully compatible with a model where the indigo molecules close the entrance to the tunnel, as originally proposed by Hubbard et al. [6], and possibly penetrate inside the tunnels [13, 17, 23–25].

Some other results can be withdrawn from our study:

- A "moderate" thermal treatment (120 °C during 90 min) is enough to stabilize MB. This is in good agreement with experimental results of Reyes-Valerio and co-authors [8, 35] and also indicates that more intense treatments proposed by other authors are not necessary.
- The surface silanols are not modified in the presence of indigo and rehydrate fully after MB formation, a result that is incompatible with the description of MB as a "surface compound," as suggested in some works [18, 21].
- There is a partial rehydration of the tunnels of MB observed by the coexistence of dry and wet signatures in the NIR bands related to octahedral cations. The rehydration is complete for raw palygorskite.
- The NH functional groups do not play a fundamental role in the MB formation. Their Raman signatures decrease linearly with temperature and do not exhibit the sigmoidal trend of the chromophore bands.
- The MIR octahedral bands in palygorskite and palygorskite–indigo show the same shift when samples are dehydrated. This shift is reversible in palygorskite and irreversible in MB, as a result of the blocking of the rehydration. The shift is only due to the hydration, and not to a possible indigo–clay interaction via the octahedral cations. The possible interaction of indigo with octahedral cations in MB has recently received a considerable attention. It has been proposed that indigo could mostly bond to Al^{3+} rather than Mg^{2+} [26]. This interaction is supposed to play a capital role in the indigo–clay association [20, 21]. However, the association clay–indigo via the octahedral Al^{3+} seems improbable (if not completely inexistent), because there is no evidence that this cation can occupy the external octahedral positions at the tunnel edges [12]. Nuclear magnetic Resonance measurements confirmed the inactivity of Al^{3+} in the clay–indigo association [31, 32].

Our results from different experimental techniques point to the model for an indigo–palygorskite complex where the indigo molecules are trapped inside the tunnels because of the similar width of the indigo (4.96 Å) and palygorskite tunnel (3.7 Å × 6.4 Å). Whether a single indigo molecule is trapped at the entrance of each tunnel, a dimer of cluster of indigo molecules blocks the entrance of each single tunnel, or several indigo monomers enter in each tunnel is a question that requires further study. Based on the presently available data, it is deduced that the indigo molecules must fill at least the opening of the tunnels in order to block rehydration. This structural anchoring is accompanied by an indigo–clay chemical interaction, which does affect the indigo chromophore. Indigo links to palygorskite through its C=O group. The changes observed in the double bonds C=O and C=C are essential in MB formation, in good agreement with numerical simulations [23, 25]. Other interactions involving N–H [23, 25] and possibly the aromatic rings with the silicon atoms of the tetrahedral sheet [31] are not excluded, but are believed to be much less important. The particular cross dimension of the palygorskite channel, which is very close to the width of the indigo molecule, and the shrinkage resulting from zeolitic dehydration are fundamental in letting the indigo to anchor in a particular position, probably via both C=O groups, which is not possible in the larger tunnel opening in sepiolite.

It has also been shown that the simultaneous use of multiple techniques is of great help for obtaining new results, in particular with MB, a complex highly studied and debated during the last years. Further study is needed to better identify the chemical mechanisms of the stability of the MB, as well as to obtain a more accurate structural model of how indigo places in palygorskite. For that, in situ studies during the necessary thermal treatment for the synthesis of MB, as presented here, will be of great help for explaining the high stability of MB.

Acknowledgements We acknowledge the ESRF for beamtime used for this experiment, and the experimental staff of BM01B for technical support and helpful discussions. Financial support from the Spanish CICYT (project CGL2006-09843) and Italian PRIN edition 2007 is also acknowledged.

References

1. Arnold DE, Bohor BF (1975) Archaeology 28:23
2. Gettens RJ (1962) Am Antiquity 7(4):557
3. Shepard AO (1962) Am Antiquity 27:565
4. Gómez-Romero P, Sanchez C (2005) N J Chem 29:57
5. Doménech A, Doménech-Carbo MT, Vázquez de Agredos Pascual ML (2006) J Phys Chem B 110(12):6027
6. Hubbard B, Kuang W, Moser A, Facey GA, Detellier C (2003) Clays Clay Miner 51(3):318
7. Reinen D, Köhl P, Müller C (2004) Zeitschrift für anorganische und allgemeine Chemie 630(1):97
8. Sanchez del Rio M, Martinetto P, Reyes-Valerio C, Dooryhée E, Suárez M (2006) Archaeometry 48(1):115
9. Bauer H, Kowski K, Kuhn H, Lüttke W, Rademacher P (1998) J Mol Struct 445(1–3):277
10. Klessinger M (1982) Dyes Pigm 3:235
11. Süsse P, Steins M, Kupcik V (1988) Z Kristallogr 184:269
12. Chryssikos GD, Gionis V, Kacandes GH, Stathopoulou ET, Suarez M, Garcia-Romero E, Sanchez del Rio M (2009) Am Miner 94(1):200
13. Chiari G, Giustetto R, Ricchiardi G (2003) Eur J Miner 15(1):21
14. Chisholm JE (1992) Can Miner 30:61
15. Post JE, Heaney PJ (2008) Am Miner 93(4):667
16. Van Olphen H (1966) Science 154:645
17. Kleber R, Masschelein-Kleiner R, Thissen J (1967) Stud Conserv 12(2):41
18. Chianelli RR, Perez De la Rosa M, Meitzner G, Siadati M, Berhault G, Mehta A, Pople J, Fuentes S, Alonzo-Nunez G, Polette LA (2005) J Synchrotron Radiat 12(2):129
19. Chiari G, Giustetto R, Druzik J, Doehne E, Ricchiardi G (2008) Appl Phys A Mater Sci Process 90(1):3
20. Fuentes ME, Contreras BPC, Montero AL, Chianelli R, Alvarado M, Olivas R, Rodríguez LM, Camacho H, Montero-Cabrera LA (2008) Int J Quantum Chem 108(10):1664
21. Manciu FS, Reza L, Polette LA, Torres B, Chianelli RR (2007) J Raman Spectrosc 38(9):1193
22. Polette-Niewold LA, Manciu FS, Torres B, Alvarado M Jr, Chianelli RR (2007) J Inorg Biochem 101(11–12):1958
23. Fois E, Gamba A, Tilocca A (2003) Microporous Mesoporous Mater 57(3):263
24. Giustetto R, Levy D, Chiari G (2006) Eur J Miner 18:629
25. Giustetto R, Llabrés i Xamena FX, Ricchiardi G, Bordiga S, Damin A, Gobetto R, Chierotti MR (2005) J Phys Chem B 109(41):19360
26. Tilocca A, Fois E (2009) J Phys Chem C 113(20):8683
27. Doménech A, Doménech-Carbó MT, Sánchez del Río M, Vázqued de Agredos Pascual ML (2009) J Solid State Electrochem 13:869
28. Doménech A, Doménech-Carbó MT, Vázqued de Agredos Pascual ML (2007) J Solid State Electrochem 11(9):1335
29. Doménech A, Doménech-Carbo MT, Vázquez de Agredos Pascual ML (2007) J Phys Chem C 111(12):4585
30. Doménech A, Doménech-Carbo MT, Vázquez de Agredos Pascual ML (2007) Anal Chem 79(7):2812
31. Doménech A, Doménech-Carbó MT, Sánchez del Río M, Goberna S, Lima E (2009) J Phys Chem C 113:12118
32. Doménech A, Doménech-Carbo MT, Sánchez del Río M, Vázquez de Agredos Pascual ML, Lima E (2009) N J Chem. doi:10.1039/b901942a
33. Boccaleri E, Carniato F, Croce G, Viterbo D, van Beek W, Emerich H, Milanesio M (2007) J Appl Crystallogr 40(4):684
34. Sanchez del Rio M, Suarez M, Garcia-Romero E (2009) Archaeometry 51(2):214
35. Reyes-Valerio C (1993) De Bonampak al Templo Mayor. El azul maya en Mesoamerica. Colección America Nuestra, vol 40. Siglo XXI Editores, Mexico D.F., p 157
36. Gionis V, Kacandes GH, Kastritis ID, Chryssikos GD (2006) Am Miner 91:1125
37. Suarez M, Garcia Romero E, Sanchez del Rio M, Martinetto P, Dooryhee E (2007) Clay Miner 42:287
38. Hayashi H, Otsuka R, Imai N (1969) Am Miner 53:1613
39. VanSoyoc GE, Serna CJ, Ahlrichs JL (1979) Am Miner 64:215
40. McKeown DA, Post JE, Etz ES (2002) Clays Clay Miner 50(5):667
41. Witke K, Brzezinka K-W, Lamprecht I (2003) J Mol Struct 661–662:235
42. Sanchez del Rio M, Picquart M, Haro-Poniatowski E, van Elslande E, Uc VH (2006) J Raman Spectrosc 37:1053
43. Tatsch E, Schrader B (1995) J Raman Spectrosc 26(6):467
44. Nagasawa Y, Taguri R, Matsuda H, Murakami M, Ohama M, Okada T, Miyasaka H (2004) Phys Chem Chem Phys 6:5370
45. Leona M, Casadio F, Bacci M, Picollo M (2004) JAIC 43:39
46. Gionis V, Kacandes GH, Kastritis ID, Chryssikos GD (2007) Clays Clay Miner 55:543
47. Jones BF, Galán E (1998) In: Bailey SW (ed) Hydrous phyllosilicates (exclusive of micas). Mineralogical Society of America, USA